Biochemical Pharmacology, Vol. 53, pp. 715–722, 1997.

ISSN 0006-2952/97/$17.00 + 0.00
PII S0006-2952(96)00906-9

Chemical Synthesis and Biological Activity of a Novel Fluorescent Etoposide Derivative

John S. Lazo, Tianhu Li,† Elizabeth S. Woo, Catherine E. Settineri, William P. Allan and Jack C. Yalowich**

Department of Pharmacology and The Experimental Therapeutics Program, University of Pittsburgh and University of Pittsburgh Cancer Institute, Pittsburgh, PA 15261, U.S.A.

ABSTRACT. The antineoplastic activity of etoposide resides in its ability to poison the nuclear enzyme DNA topoisomerase II (topo II). The factors that control the cellular entry and subcellular distribution of etoposide remain poorly understood. Therefore, we have synthesized a novel fluorescence-labeled etoposide (Bodipy-etoposide) by coupling 4,4-difluoro-5,7-dimethyl-4-bora-3a,4a-diaza-s-indacene-3-propionylethylenediamine (Bodipy) to 4′-benzyloxycarbonyl-4′-demethylepipodophyllotoxin β-D-glucopyranoside, a precursor of etoposide. Bodipy-etoposide retained the ability to stabilize topo II–DNA covalent complexes in isolated nuclei, although it was significantly less potent and efficacious than etoposide. The growth inhibitory activity of Bodipy-etoposide was also approximately 200-fold less than that of etoposide in human leukemia K562 and DU-145 prostatic carcinoma cells. Nonetheless, etoposide-resistant K/VP.5 and K/VP.5-1 leukemia cells were cross-resistant to Bodipy-etoposide compared with parental K562 cells. Analysis by flow cytometry revealed a concentration-dependent Bodipy-etoposide cell association with no significant difference in drug association in the etoposide-resistant cell lines relative to the parental K562 cells. Using confocal laser scanning microscopy, we found significant cytoplasmic perinuclear localization of Bodipy-etoposide. Thus, Bodipy-etoposide displays promise as a tool to probe the factors controlling entry and subcellular distribution of etoposide-like compounds in live cells. BIOCHEM PHARMACOL 53;5:715–722, 1997. © 1997 Elsevier Science Inc.

KEY WORDS. fluorescent drug; tumor cells; drug resistance; topoisomerase; etoposide

Natural products and their synthetic derivatives are among the most commonly used anticancer agents. In general, they have chemical structures more complex and larger than most pharmaceuticals. In addition, they frequently have intracellular targets and, thus, must enter cells to act. Perhaps because of their size and chemical complexity, we know surprisingly little about the intracellular trafficking of natural products. Indeed, one common cause of resistance to the natural products in both prokaryotes and eukaryotes appears to be decreased cellular drug accumulation; this may be through altered drug influx and/or efflux [1].

Etoposide,‡ which is structurally related to the natural product podophyllotoxin, is now one of the most extensively used anticancer drugs. Both etoposide and its more lipophilic analog, teniposide, are thought to act by poisoning DNA topoisomerase II [2]. The mechanism of cellular uptake, efflux, and the modes by which etoposide and teniposide reach their nuclear target are not well characterized. Intracellular teniposide concentrations have been reported to be 20-fold higher than that of the extracellular medium, whereas etoposide concentrations are only 2-fold [3]. Results from several laboratories using relatively low specific activity radiolabeled etoposide suggest that alterations in drug uptake, efflux, or subcellular distribution are important in etoposide and teniposide resistance [4–7].

Advances in fluorescence chemistry and instrumentation permit the generation and analyses of fluorescent analogues of relatively small molecular weight antieoplastic agents that are useful in studying localization of live cells. We previously synthesized and characterized a fluorescent bleomycin analogue that appears to simulate at least some of the uptake properties of the natural compound [8, 9]. The cellular uptake and distribution of this agent could be visualized microscopically in live cells. We now describe the synthesis and initial biochemical and biological characterization of a fluorescence-labeled etoposide/teniposide analog.

* Corresponding authors: John S. Lazo and Jack C. Yalowich, Department of Pharmacology, 10th Floor, Biomedical Science Tower, University of Pittsburgh School of Medicine, Pittsburgh, PA 15261. Tel. (412) 648-9420; FAX (412) 648-1945; E-mail: lazo@pop.pitt.edu or yalowich+@pitt.edu

† Current address: Department of Chemistry, The Scripps Research Institute, MB 10A, 10666 North Torrey Pines Road, La Jolla, CA 92037.

‡ *Abbreviations:* Bodipy, 4,4-difluoro-5,7-dimethyl-4-bora-3a,4a-diaza-s-indacene-3-propionylethylenediamine; etoposide, 4′-demethylepipodophyllotoxin-9-(4,6-O-ethylidene-β-D-glucopyranoside); teniposide, 4′-demethylepipodophyllotoxin-9-(4,6-O-2-thenylidene-β-D-glucopyranoside); MTT, 3-(4,5-dimethylthiazol-2-yl)-2,5-diphenyltetrazolium bromide; and TsOH, *p*-toluenesulfonyl hydroxide.

Received 3 September 1996; accepted 17 October 1996.

MATERIALS AND METHODS

Chemistry

GENERAL METHODS. Reagents for chemical syntheses were obtained commercially and used without further purification. All reactions were monitored by TLC carried out on 0.25 mm E. Merck silica gel plates (60F-254) using UV light. Preparative TLC was performed on 0.5 mm × 20 cm × 20 cm E. Merck silica gel plates (60F-254). ^{1}H NMR spectra were recorded on a Bruker AM-300 or AMX-500 instrument. High resolution mass spectra were recorded on a VG ZAB-2SE mass spectrometer.

PREPARATION OF (5). To a solution of 4′-benzyloxycarbonyl-4′-demethylepipodophyllotoxin β-D-glucopyranoside **(4)** (15 mg, 21 μmol) in CH_3NO_2 (3 mL) was added succinimidyl *p*-formylbenzoate **(3)** (40 mg, 160 μmol; Molecular Probes, Inc. Eugene, OR) and TsOH (approximately 1 mg), and the reaction mixture was stirred under N_2 at room temperature for 2 hr. Preparative TLC ($CHCl_3$:CH_3OH = 10:1) of the reaction mixture produced **(5)** (13 mg, 14 μmol, 65.6%). ^{1}H NMR (DMSO-d_6) δ 2.94 (s, 4H), 3.67 (s, 6H), 4.32 (d, 1H), 4.65 (m, 1H), 4.98 (s, 1H), 5.23 (s, 2H).

PREPARATION OF (6). To a suspension of Bodipy (20 mg, 30 μmol) and **(5)** (10 mg, 10 μmol) in CH_3NO_2 (2 mL), we added a few drops of triethylamine, and the mixture was stirred at room temperature for 2 hr. The brown-colored reaction mixture was purified by preparative TLC ($CHCl_3$:CH_3OH = 15:1) to afford **(6)** (1.5 mg, 1.3 μmol, 10.8%). ^{1}H NMR (DMSO-d_6) δ 3.59 (s, 6H), 3.74 (t, 1H), 4.26 (t, 3H), 4.60 (t, 3H), 4.95 (d, 1H), 5.26 (s, 2H), 5.32 (m, 2H), 5.62 (s, 1H), 6.01 (s, 2H), 6.30 (m, 4H), 6.53 (s, 1H), 7.02 (s, 2H), 7.34 (m, 5H), 7.51 (d, 2H), 7.65 (s, 1H), 7.83 (d, 2H), 8.06 (t, 1H), 8.52 (t, 1H).

PREPARATION OF (2). Palladium on activated carbon (Pd 10%) (50 mg) was added to a solution of **(6)** (3 mg, 2.6 μmol) in methyl acetone:water (5:1) (1.5 mL). The mixture was stirred at room temperature for 0.5 hr under an H_2 atmosphere. Solid catalyst was filtered off, and the filtrate was purified further by preparative TLC ($CHCl_3$:CH_3OH = 20:1) of the reaction mixture to afford **(2)** (1.5 mg, 1.5 μmol, 56.7%). ^{1}H NMR (DMSO-d_6) δ 3.60 (s, 6H), 3.89 (m, 1H), 4.22 (m, 3H), 4.59 (m, 3H), 4.72 (m, 2H), 5.18 (s, 2H), 5.45 (m, 3H), 5.68 (s, 1H), 6.18 (d, 2H), 6.27 (s, 2H), 6.38 (m, 1H), 6.65 (m, 2H), 7.57 (d, 2H), 7.74 (s, 1H), 7.80 (d, 2H), 8.38 (t, 1H), 8.54 (s, 1H), 8.79 (t, 2H). MS: 1010 (25%), 968 (100). ^{13}C NMR (DMSO-d_6 δ 175.0, 171.4, 166.3, 159.1, 158.0, 148.0, 147.3, 146.4, 144.4, 140.8, 135.2, 134.9, 138.0, 133.0, 130.8, 129.9, 129.2, 127.3, 126.4, 125.6, 120.5, 116.8, 110.1, 108.5, 101.7, 101.5, 100.3, 80.86, 74.5, 73.5, 72.0, 67.9, 66.0, 56.2, 43.2, 38.5, 37.4, 34.0, 31.9, 24.2, 14.8, 11.2. High resolution fast atom bombardment mass spectroscopy, calculated for $C_{51}H_{53}O_{15}N_4F_2B$: *m/z* 1010.3625; found 1010.3626.

Biology

CELL CULTURE. Human DU-145 prostatic carcinoma cells (American Type Culture Collection, Rockville, MD) were cultured in RPMI-1640 medium (GIBCO/BRL, Gaithersburg, MD) containing 10% fetal bovine serum (HyClone, Logan, UT), 100 U/mL penicillin G sodium, and 100 μg/mL streptomycin sulfate (GIBCO/BRL), as previously described [10]. Cells were tested routinely and found to be free of mycoplasma contamination. The antiproliferative activities of etoposide and Bodipy-etoposide were determined with exponentially growing DU-145 cells using the well-established microtiter colorimetric assay based on the reduction of MTT [11]. Cells were cultured in 96-well plates, for 24 hr and treated continuously with 0–30 μM drug at 37°. After 72 hr, 100 μL of MTT (1 mg/mL) was added, and cells were incubated in the dark and 5% CO_2 for 3 hr at 37°. MTT was replaced with 100 μL DMSO and shaken for 5 min at room temperature. Absorbance at 540 nm was determined with a Titertek Multiskan Plus plate reader. Each experiment was performed in triplicate three times.

Human K562 cells and the etoposide-resistant K/VP.5 and K/VP.5-1 cells were grown in suspension in Dulbecco's Modified Eagle's Medium supplemented with 10% fetal bovine and 2 mM L-glutamine as previously described [12]. All cells were cultured at 37° under an atmosphere of 95% air and 5% CO_2. Exponentially growing K562 and etoposide-resistant K562 cells (5×10^5 cells/mL) were incubated continuously for 48 hr with 0–20 μM etoposide or 0–100 μM Bodipy-etoposide, and the total number of cells was determined using a ZF Coulter counter (Coulter Electronics, Hialeah, FL) as described previously [12]. The extent of growth in drug-treated versus untreated control cells was expressed as percent inhibition of untreated control cell growth.

FLOW CYTOMETRY. K562, K/VP.5, and K/VP.5-1 cells (5×10^5/mL) were incubated at 37° for various times with 0–20 μM Bodipy-etoposide, washed twice with drug-free medium, and analyzed by flow cytometry with a Becton Dickinson FACStar with respect to their red fluorescence profile (excitation, 503 nm; emission, 530 nm). Experiments were performed at least two independent times.

CONFOCAL MICROSCOPY. Exponentially growing DU-145 (1×10^5) cells were harvested and plated in 35-mm tissue culture dishes that contained sterile glass cover slips and the above-mentioned medium for DU-145 cells. Bodipy-etoposide or Bodipy-paclitaxel were resuspended in DMSO as 400 μM solutions. Attached DU-145 cells were washed and incubated with a prewarmed (37°) medium containing 0–100 μM Bodipy-etoposide or 20 μM Bodipy-paclitaxel for 2 min. Then cells were quickly washed three times and immediately reincubated with Hanks' Balanced Salt Solution and examined with repetitive 1-min scans using a Meridian ACAS 570c laser confocal microscope having a 100 μm pinhole and 0.4 μm confocal Z axis step size as described previously [8].

TOPOISOMERASE II–DNA COVALENT COMPLEXES. Topoisomerase II–DNA covalent complex formation in isolated

nuclei was measured as previously described [13]. Briefly, exponentially growing K562 cells were labeled for 24 hr with 0.5 mCi/mL [*methyl*-^{3}H]thymidine (0.5 Ci/mmol) and 0.1 mCi/mL [U-^{14}C]leucine (320 mCi/mmol). For isolation of nuclei, cells were washed in ice-cold buffer A (1 mM KH_2PO_4, 5 mM $MgCl_2$, 150 mM NaCl, 1 mM EGTA, pH 6.4). Cells were then resuspended in 1 mL of buffer A, lysed by the addition of 9 mL of buffer B (0.3% Triton X-100 in buffer A), and incubated on ice for 30 min [14]. After lysis, 40 mL of buffer A was added, and nuclei were pelleted by centrifugation at 350 *g* for 10 min in an IEC model HN-SII tabletop centrifuge. The density of nuclei was adjusted to 1 × 10^6/mL in 37°, pH 7.4, buffer A containing 1 mM ATP for experiments. Isolated nuclei were then incubated for 30 min with various concentrations of etoposide, Bodipy-etoposide, or 0.1% DMSO solvent (control). Reactions were stopped by adding 1 mL nuclei suspension to 10 mL of ice-cold PBS. Nuclei were then pelleted and lysed, cellular DNA was sheared, and protein–DNA complexes were precipitated with SDS and KCl as described [15]. Topoisomerase II–DNA covalent complexes were quantified by scintillation counting, and [^{3}H]DNA was normalized to cell number using the co-precipitated ^{14}C-labeled protein as an internal control.

REAGENTS. Bodipy-paclitaxel (10 μg; FL conjugate P-7500) was a gift from Dr. David J. Phelps (Molecular Probes, Inc., Eugene, OR). The 4′-benzyloxycarbonyl-4′-demethylepipodophyllotoxin β-D-glucopyranoside **(4)** was a gift from Dr. Byron Long (Bristol Myers Squibb, Princeton, NJ).

RESULTS

Extensive structure–activity studies with etoposide analogues indicate that epipodophyllotoxin tolerates very few structural modification without affecting its activity. Consequently, the *trans* fused lactone ring, the *trans* configuration between 1-β-D-glucopyranoside and the 4-α-(3′,5-dimethoxy-4-hydroxy)phenyl ring, and the dimethoxyphenol ring are essential [16]. Thus, we selected the β-D-glucopyranoside ring present on 4′-demethyl-epipodophyllotoxin as the moiety to modify for the synthesis of a fluorescent etoposide analogue. This site is modified in teniposide compared with etoposide and, therefore, we hoped to retain at least some antitopoisomerase II activity. Bodipy was selected as the fluorophore because it has spectral properties similar to fluorescein, has a better fluoresent intensity than fluorescein, retains good fluorescent properties over physiologically relevant pH ranges, is not quenched in H_2O, is uncharged, is relatively small in molecular mass, has good hydrophillic properties, and has been used successfully to produce fluorescent small molecules, namely Bodipy-verapamil [17] and Bodipy-paclitaxel (Molecular Probes, Inc.). The comparative chemical structures of both etoposide and Bodipy-etoposide are shown in Fig. 1. Starting with 4′ benzyloxycarbonyl-4′-demethylepipodophyllotoxin β-D-glucopyranoside **(4)** and succinimidyl *p*-formylbenzoate **(3)**, we prepared **(5)** with a yield of 66% (Scheme 1). Subsequent coupling of BODIPY to **(5)** resulted in the Bodipy-etoposide precursor **(6)**. Deprotection with palladium on activated carbon under H_2 resulted in the formation of the final product, Bodipy-etoposide **(2)**, with a 57% yield. The chemical structure and purity of **(2)** were confirmed by high resolution mass spectroscopy, ^{1}H NMR, and ^{13}C NMR.

We next determined the pharmacological activity of Bodipy-etoposide using a colorimetric cell culture growth inhibition assay. Continuous exposure of human DU-145 prostatic carcinoma cells to etoposide resulted in a concentration-dependent inhibition of growth (Fig. 2). At approximately 3 μM etoposide, 50% growth inhibition was

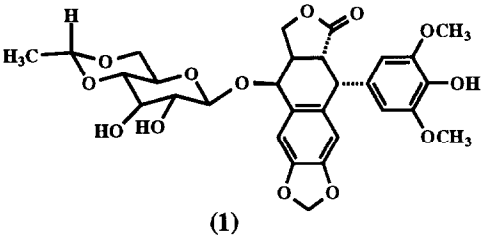

(1)

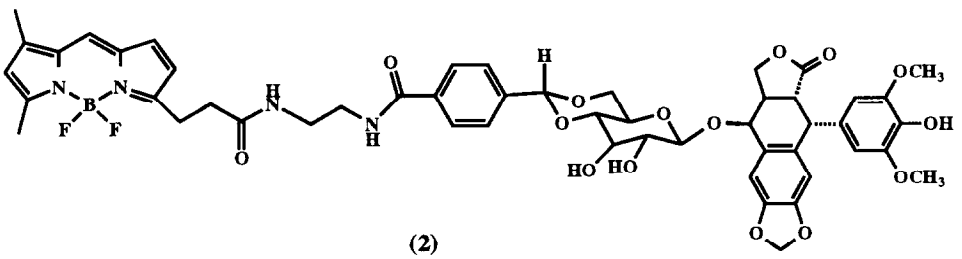

(2)

FIG. 1. Structures of etoposide (1) and Bodipy-etoposide (2).

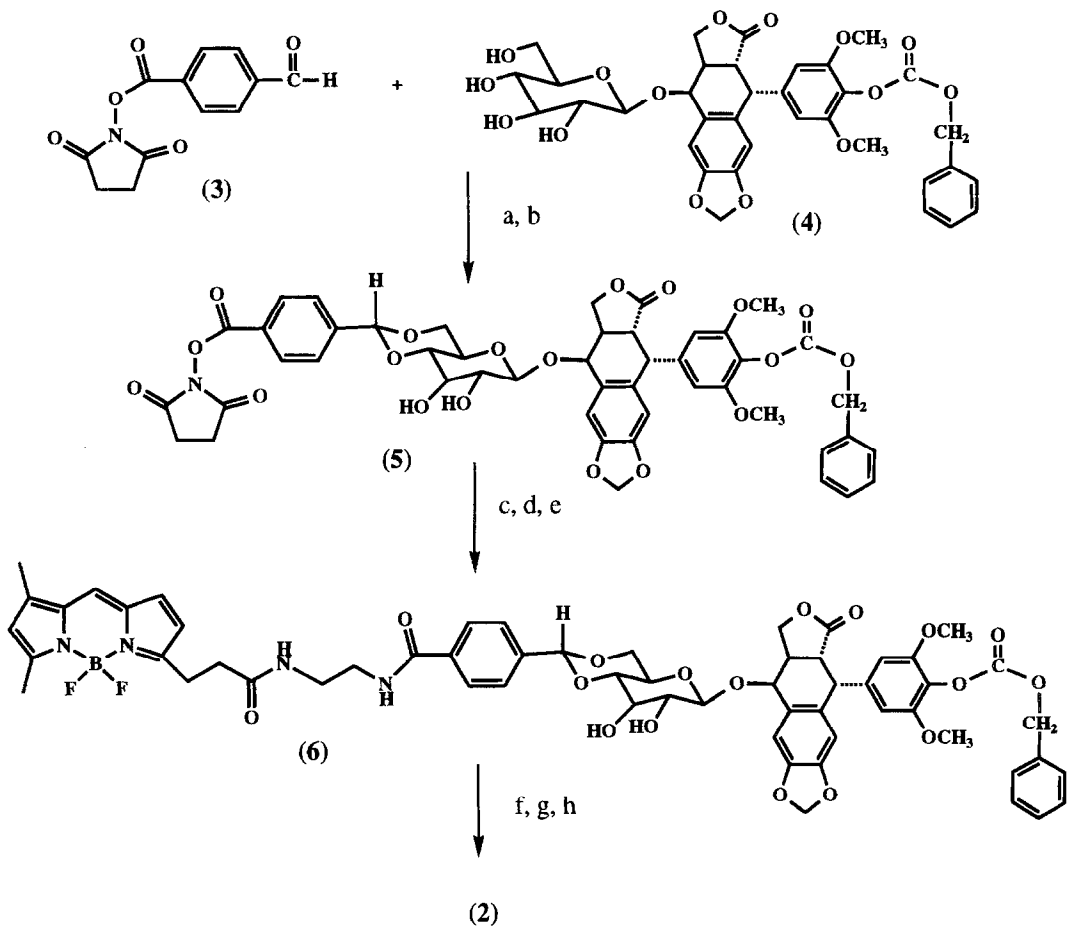

Scheme I. Synthetic route used to generate Bodipy-etoposide (2). Reagents used were: (a) CH_3NO_2; (b) TsOH; (c) CH_3NO_2; (d) triethylamine; (e) BODIPY; (f) $(CH_3)_2CO$; (g) Pd-C; and (h) H_2. Additional details are provided in Materials and Methods.

seen with DU-145 cells, while no significant growth inhibition was seen with up to 300 μM Bodipy-etoposide (Fig. 2). Similarly, K562 cells were approximately 200-fold less sensitive to the growth inhibitory activity of continuous exposure of Bodipy-etoposide compared with etoposide (Fig. 3, A and B). Nonetheless, the two etoposide-resistant cell lines derived from K562 cells were cross-resistant to Bodipy-etoposide, with K/VP.5-1 cells being slightly more resistant than K/VP.5 cells at most concentrations (Fig. 3B), thus recapitulating what has been observed with etoposide and these resistant cells [12, 18] (Fig. 3A). These results suggest that Bodipy-etoposide, while significantly less potent than etoposide, retained some pharmacological properties similar to etoposide.

To investigate this issue further, we compared Bodipy-etoposide with etoposide with respect to its ability to induce covalent protein–DNA complexes with isolated nuclei, an indirect measurement of topoisomerase II poisoning. A concentration-dependent increase in topoisomerase II–DNA complexes was seen with etoposide, with 20 μM etoposide producing almost a 4-fold increase (Fig. 4). Bodipy-etoposide was less potent and efficacious as a topoisomerase II inhibitor with an approximate 2-fold increase at 20 μM (Fig. 4).

To examine the cell accumulation of Bodipy-etoposide, we incubated K562 cells with 20 μM Bodipy-etoposide for various times and determined fluorescence by flow cytometry (Fig. 5). K562 cells had detectable autofluorescence in the spectral range of fluorescein but even a 0.1-min incubation with Bodipy-etoposide resulted in a marked increase in cell fluorescence (Fig. 5). Accumulation was rapid with maximum cell association apparent by 10 min. This is similar to the previously described cellular uptake rate of radiolabeled etoposide in K562 cells [18, 19]. The cellular fluorescence was dependent on the extracellular concentration (Fig. 6). We were unable to detect a reproducible difference in the cellular fluorescence with Bodipy-etoposide using K562, K/VP.5, or K/VP.5-1 cells (data not shown). We also examined whether coincubating K562 cells with etoposide and Bodipy-etoposide would affect the cell-associated fluorescence. Due to the limited solubility of etoposide, we were only capable of using a 10-fold excess of unlabeled etoposide and saw no effect on cell-associated Bodipy-etoposide fluorescence (data not shown).

To distinguish between cell surface binding and intracellular incorporation, we incubated live attached DU-145 cells with Bodipy-etoposide for 2 min at 37° and examined the subcellular localization after three rapid washings with

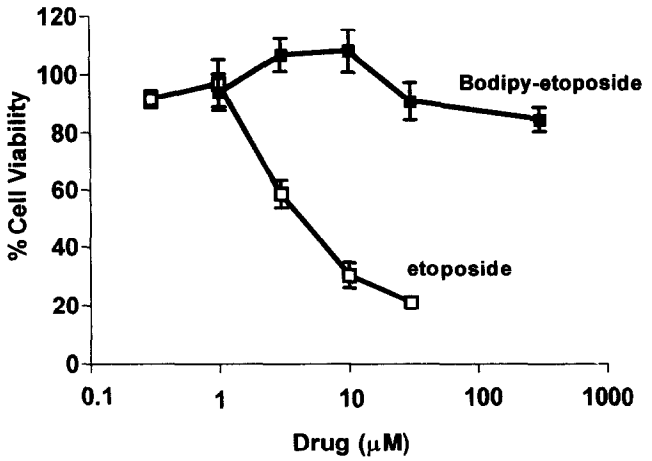

FIG. 2. Comparative growth inhibitory effects of etoposide and Bodipy-etoposide in humn DU-145 prostatic carcinoma cells. Exponentially growing cells were incubated for 3 days with various concentrations of etoposide (□) or Bodipy-etoposide (■), and cell numbers were determined by the MTT assay. Each value is the mean ± SEM of three independent determinations.

Hanks' Balanced Salt Solution. Using confocal microscopy, we were required to use concentrations of 100 μM Bodipy-etoposide to detect a sufficiently strong signal. The drug was clearly localized within the cells with no evidence of significant surface binding (Fig. 7). This was also confirmed by multiple serial sections (0.4 μm) with DU-145 cells (data not shown). The fluorescence was sequestered in the perinuclear region and was distinctly absent from the nucleus (Fig. 7). We saw little change in the distribution of the fluorescence even after 15 min incubation in drug-free medium. In contrast, we were able to detect readily the subcellular distribution of 20 μM Bodipy-paclitaxel, which had a slightly more cytoplasmic localization than Bodipy-etoposide (data not shown). Unfortunately, we had insufficient quantities of Bodipy-paclitaxel to examine this agent at a concentration of 100 μM to allow for a direct comparison with Bodipy-etoposide.

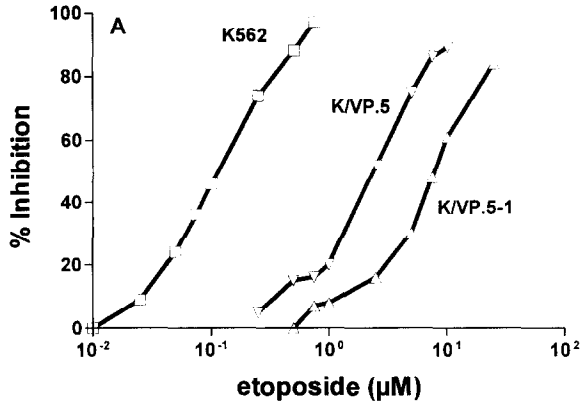

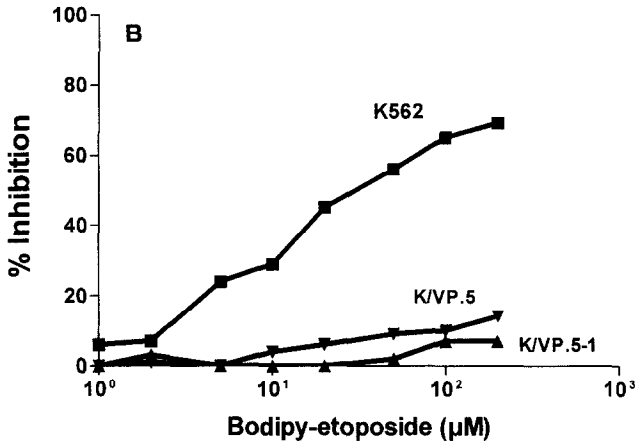

FIG. 3. Growth inhibition of etoposide and Bodipy-etoposide with K562 cells and etoposide-resistant K562 cell lines. Cells were incubated for 48 hr with various concentrations of either etoposide (open symbols) or Bodipy-etoposide (closed symbols). Total cell number was determined with a Coulter Counter, normalized to the untreated control cell number, and expressed as percent inhibition of cell growth. Panel A: etoposide; Panel B: Bodipy-etoposide. Key: K562 (□,■); K/VP.5 (▽,▼); and K/V.5-1 (△,▲).

DISCUSSION

Most therapeutic agents do not require cellular entry to function. In contrast, almost all currently useful anticancer drugs have intracellular targets. Fluorescent analogues of peptides, hormones, and drugs have proven to be valuable alternatives to radiolabeled species for studying the processes of cellular internalization and intracellular trafficking. Methotrexate covalently linked to fluorescein has been used to identify and select cells with methotrexate transport deficiencies [20]. Dansylated estramustine has been used as a fluorescent probe to examine cellular uptake and distribution of estramustine in live human prostatic cells [21]. The entry mechanisms and subcellular distribution of natural product anticancer agents, which are derived from marine and plant sources, have been more difficult to study because of their greater mass and chemical complexity. Several natural products have been radiolabeled, but generally they have a low specific activity that limits their utility. Furthermore, radiolabeling does not readily permit tracking the movement of agents within live cells in real time. Some natural products have sufficient intrinsic fluorescence to permit monitoring intracellular movement. Thus, intracellular distribution of daunorubicin has been studied by fluorescent light microscopy in living human KB cells and found to be primarily in the nucleus but also in the organelles of the Golgi region and in lysosomes [22]. Intracellular daunorubicin appeared markedly decreased in multidrug-resistant KB cells with a noticeable lack of nuclear fluorescence [22]. Previously, we synthesized a fluorescein-labeled derivative of the bleomycin analogue talisomycin S_{10b} and found that human tumor cells resistant to bleomycin were

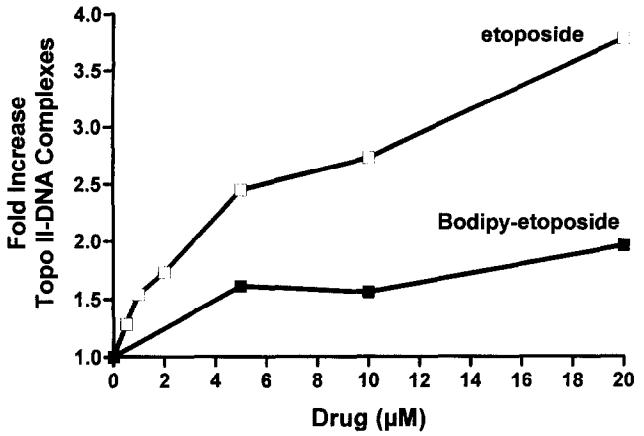

FIG. 4. Formation of topoisomerase II–DNA covalent complexes in K562 nuclei treated with etoposide (□) or Bodipy-etoposide (■). Nuclei from cells prelabeled with [*methyl*-^{3}H]thymidine and [U-^{14}C]leucine were incubated for 30 min in the presence of the indicated concentrations of drug and 1 mM ATP. Potassium chloride-SDS-precipitable DNA complexes were isolated and quantified as described in Materials and Methods. Results are expressed as fold-increase in drug-induced topoisomerase II–DNA complexes relative to complexes isolated from nuclei incubated in the absence of drug. Each result is the mean of at least two independent determinations with less than 20% difference from the mean value.

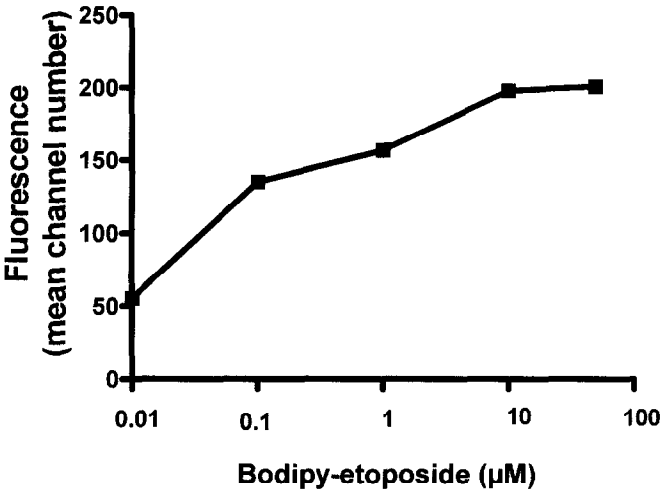

FIG. 6. Concentration-dependent cell association of Bodipy-etoposide. K562 cells were incubated with various concentrations of Bodipy-etoposide for 30 min, washed, and analyzed by flow cytometry as described in Materials and Methods. Each value is the mean channel number obtained from two independent experiments; the range did not exceed the size of the symbols.

cross-resistant to the fluorescent bleomycin analogue [8]. In human head and neck cells, there was heterogenous distribution of fluorescence with approximately 50% of the cells exhibiting marked nuclear fluorescence [8, 9]. The chemical modifications associated with the attachment of the fluorophore did not alter the DNA cleavage profile of the fluorescent compound compared with talisomycin S_{10b}, although the fluorescent derivative was markedly less potent than the unaltered compound [23]. Similarly, fluorescent bleomycin was approximately 25-fold less potent as an antiproliferative agent against human head and neck squamous carcinoma cells than the unaltered compound [8].

The Bodipy fluorophore has been successfully linked to the P-glycoprotein modulator verapamil and used to ex-

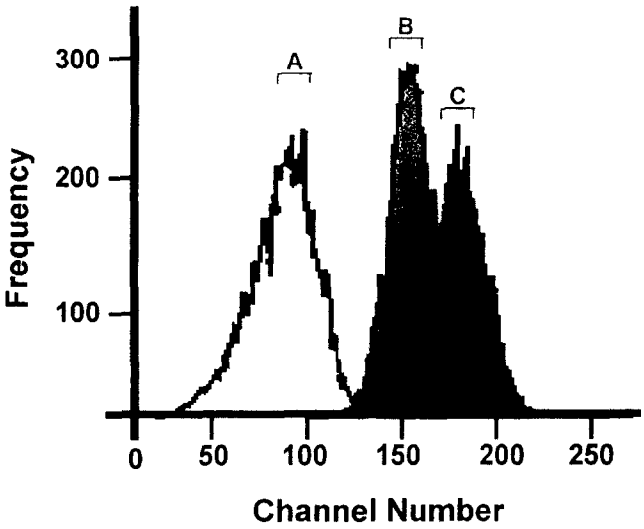

FIG. 5. Flow cytometry profiles of K562 cells after incubation with or without Bodipy-etoposide. K562 cells (1×10^6 cells/mL) were incubated with vehicle (control; profile A), or 20 μM Bodipy-etoposide for 0.1 (profile B; gray), or 10 min (profile C; black). Cells were washed three times with ice-cold serum-free medium (14,000 *g* for 1 min) and resuspended in drug-free medium. Cells were examined twice with similar results.

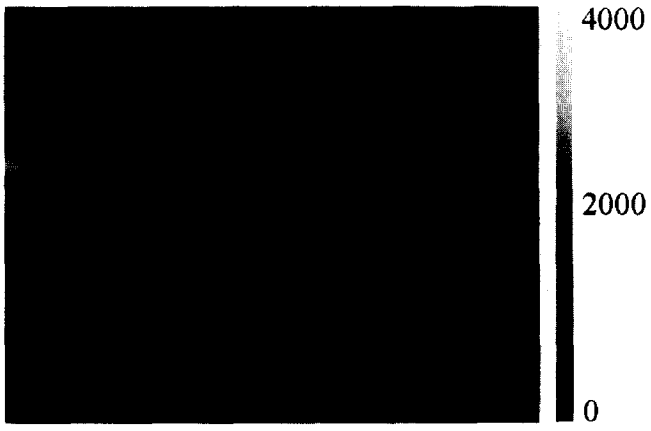

FIG. 7. Subcellular distribution of Bodipy-etoposide. DU-145 cells (1×10^5) were plated on glass cover slips and incubated with Hanks' Balanced Salt Solution containing 100 μM Bodipy-etoposide for 2 min. Cells were washed and then examined with a Meridian ACAS 570c confocal microscope as described in Materals and Methods. The gray scale output is located on the right and was assigned arbitrary fluorescent units.

plore drug efflux [17]. Bodipy-verapamil accumulates in lysosomes of NIH3T3 and KB cells but is effluxed more rapidly from multidrug-resistant P-glycoprotein expressing derivatives of NIH3T3 and KB cell lines than from the wild type cells. These studies demonstrate that Bodipy can be added to a small molecule without completely disrupting the biological or pharmacological activity. Although Bodipy-verapamil appears to be a substrate for the multidrug transporter, it is less efficient than verapamil as a reversal agent against vinblastine and colchicine resistance [17]. Interestingly, the Bodipy-verapamil itself seems more toxic to cells than verapamil. In contrast, we found that the fluorescent derivative of talisomycin S_{10b} [8] and Bodipy-etoposide lost a significant fraction of their antiproliferative activity compared with the unmodified compound. Thus, it is difficult to predict *a priori* how the actions of a small molecule will be altered after the addition of a relatively small fluorophore. Loss of antiproliferative activity, however, could afford advantages as higher concentrations of the probe can be used without the appearance of toxicity.

Bodipy-etoposide retained some antitopoisomerase II activity but lost both potency and efficacy (Fig. 4). Although we have not established that Bodipy-etoposide kills cells by poisoning topoisomerase II, it is a reasonable hypothesis and may explain the difference in growth inhibition of etoposide and Bodipy-etoposide. Furthermore, the cross-resistance profiles in K562 cells with altered topoisomerase also are consistent with the hypothesis that topoisomerase II is an intracellular target for Bodipy-etoposide. Bodipy-etoposide is clearly taken up by mammalian cells. The kinetics are consistent with that previously seen with radiolabeled etoposide [5, 18, 19], and the cellular content was dependent on the extracellular concentration (Fig. 6). Interestingly, we did not observe any significant difference in the fluorescent drug content in the K562-derived etoposide-resistant cells, which is consistent with current information with K/VP.5 cells [13]. Our preliminary data with K/VP.5-1 indicate no more than a 3-fold difference in the radiolabeled etoposide content [18].

Bodipy-etoposide appears to be located primarily in the cytoplasm after a 2-min incubation. We have not yet examined longer incubation periods. Even 10 min after removal of extracellular Bodipy-etopside, we found that the majority of fluorescence was retained in the cytoplasm. Thus, our microscopic data are in agreement with current information using radiolabeled etoposide [3, 19, 24], which suggests that most of the intracellular etoposide is located in the cytoplasm. Although the addition of a fluorophore to a ligand, especially a small molecule, such as etoposide, could alter its subcellular distribution, the apparent quantitative and qualitative differences between Bodipy-etoposide and Bodipy-paclitaxel also suggested that the ligand rather than just the fluorophore dictated the cellular uptake and distribution. An additional attractive feature of Bodipy-etoposide is its relative lack of toxicity, which could facilitate its use in live cells. Bodipy-etoposide was readily detected in mammalian cells by flow cytometry, and we believe that the fluorescent etoposide probe could have some utility for selecting cells with high or low Bodipy-etoposide content. If the drug accumulation phenotype is stable, we may obtain unique insight into the factors that control drug uptake, accumulation, and efflux without exposure to potentially toxic compounds.

We are especially grateful to Professor Ian Reynolds for his assistance with the Meridian ACAS 570c confocal microscope. This work was supported by American Cancer Society Grant DHP77 (J. S. L), DHP125 (J. C. Y.), NIH Grant CA61299 (J. S. L), NIH NRSA CA62781 (E. S. W.), the Fiske Drug Discovery Fund (J.S.L.) and Leukemia Society of America Grant 6238-95 (J. C. Y.).

References

1. Teicher BA, *Drug Resistance in Oncology*. Marcel Dekker, New York, 1993.
2. Liu L, DNA topoisomerase poisons as antitumor drugs. *Annu Rev Biochem* **58:** 351–377, 1989.
3. Allen LM, Comparison of uptake and binding of two epipodophyllotoxin glucopyranosides, 4′-demethyl epipodophyllotoxin thenylidene-β-D-glucoside and 4′-demethyl epipodophyllotoxin ethylidene-β-D-glucoside, in the L1210 leukemia cell. *Cancer Res* **38:** 2549–2554, 1978.
4. Sehested M, Friche E, Jensen PB and Demant EJF, Relationship of VP-16 to the classical multidrug resistance phenotype. *Cancer Res* **52:** 2874–2879, 1992.
5. Yalowich JC and Ross WE, Verapamil-induced augmentation of etoposide accumulation in L1210 cells *in vitro*. *Cancer Res* **45:** 1651–1656, 1985.
6. Politi PM and Sinha BK, Role of differential drug uptake, efflux, and binding of etoposide in sensitive and resistant human tumor cell lines: Implications for the mechanisms of drug resistance. *Mol Pharmacol* **35:** 271–278, 1989.
7. Long BH, Wang L, Lorico A, Wang RCC, Brattain MG and Casazza AM, Mechanisms of resistance to etoposide and teniposide in acquired resistant human colon and lung carcinoma cell lines. *Cancer Res* **51:** 5275–5284, 1991.
8. Mistry JS, Jani JP, Morris G, Mujumdar RB, Reynolds IJ, Sebti SM and Lazo JS, Synthesis and evaluation of fluoromycin: A novel fluorescence-labeled derivative of talisomycin S_{10b}. *Cancer Res* **52:** 709–718, 1992.
9. Lazo JS, Mistry JS and Sebti SM, Fluoromycin: A novel bleomycin analog. *J Cell Pharmacol* **3:** 94–97, 1992.
10. Rusnak JM, Calmels TPG, Hoyt DG, Kondo Y, Yalowich JC and Lazo JS, Genesis of discrete higher order DNA fragments in apoptotic human prostate carcinoma cells. *Mol Pharmacol* **49:** 244–252, 1996.
11. Lazo JS, Kondo Y, Dellapiazza D, Michalska AE, Choo KHA and Pitt BR, Enhanced sensitivity to oxidative stress in cultured embryonic cells from transgenic mice deficient in metallothionein I and II genes. *J Biol Chem* **270:** 5506–5510, 1995.
12. Ritke MK and Yalowich JC, Altered gene expression in human leukemia K562 cells selected for resistance to etoposide (VP-16). *Biochem Pharmacol* **46:** 2007–2020, 1993.
13. Ritke MK, Roberts D, Allan WP, Raymond J, Bergoltz VV and Yalowich JC, Altered stability of etoposide-induced topoisomerase II/DNA complexes in resistant human leukemia K562 cells. *Br J Cancer* **69:** 687–697, 1994.
14. Filipski J and Kohn KW, Ellipticine-induced protein-associated DNA breaks in isolated L1210 nuclei. *Biochim Biophys Acta* **698:** 280–286, 1982.
15. Zwelling LA, Hinds M, Chan D, Mayes J, Sie KL, Parker E,

Silberman L, Radcliffe A, Beran M and Blick M, Characterization of an amsacrine-resistant line of human leukemia cells. Evidence for a drug-resistant form of topoisomerase II. *J Biol Chem* **264:** 16411–16420, 1989.
16. Stähelin HF and von Wartburg A, The chemical and biological route from podophyllotoxin glucoside to etoposide: Ninth Cain Memorial Award Lecture. *Cancer Res* **51:** 5–15, 1991.
17. Lelong IH, Guzikowski AP, Haugland RP, Pastan I, Gottesman MM and Willingham MC, Fluorescent verapamil derivative for monitoring activity of the multidrug transporter. *Mol Pharmacol* **40:** 490–494, 1991.
18. Yalowich JC, Lush RM, Allan WP, Rabindran S and Greenberger LM, Acquired resistance to etoposide in K562 cells: Multidrug resistance associated protein overexpression occurs subsequent to changes in DNA topoisomerase II. *Proc Am Assoc Cancer Res* **37:** 2128, 1996.
19. Yalowich JC, Microtubule inhibitor effects on etoposide accumulation and DNA damage in human K562 leukemia cells *in vitro*. *Cancer Res* **47:** 1010–1015, 1987.
20. Assaraf YG and Schimke RT, Identification of methotrexate transport deficiency in mammalain cells using fluoresceinated methotrexate and flow cytometry. *Proc Natl Acad Sci USA* **84:** 7154–7158, 1987.
21. Stearns ME, Jenkins DP and Tew KD, Dansylated estramustine, a fluorescent probe for studies of estramustine uptake and identification of intracellular targets. *Proc Natl Acad Sci USA* **82:** 8483–8487, 1985.
22. Willingham MC, Cornwell MM, Cardarelli CO, Gottesman MM and Pastan I, Single cell analysis of daunomycin uptake and efflux in multidrug-resistant and -sensitive KB cells: Effects of verapamil and other drugs. *Cancer Res* **46:** 5941–5946, 1986.
23. Mistry JS, Koepsel RR and Lazo JS, Structural basis for the sequence selectivity of DNA cleavage by beomycins. *Biochem Biophys Res Commun* **191:** 420–426, 1993.
24. Ross W, Rowe T, Glisson B, Yalowich J and Liu L, Role of topoisomerase II in mediating epipodophyllotoxin-induced DNA cleavage. *Cancer Res* **44:** 5857–5860, 1984.